

Heat transport in proximity structures

E. V. Bezuglyi^{1,2} and V. Vinokur²

¹*Institute for Low Temperature Physics and Engineering, Kharkov 61103, Ukraine*

²*Argonne National Laboratory, Argonne IL 60439, U.S.A.*

(Dated: April 26, 2018)

We study heat and charge transport through a normal diffusive wire coupled with a superconducting wire over the region smaller than the coherence length. Due to partial Andreev reflection of quasiparticles from the interface, the subgap thermal flow is essentially suppressed and approaches zero along with energy, which is specific for diffusive structures. Whereas the electric conductance shows conventional reentrance effect, the thermal conductance κ rapidly decreases with temperature which qualitatively explains the results of recent experiments. In the Andreev interferometer geometry, κ experiences full-scale oscillations with the order parameter phase difference.

PACS numbers: 74.25.Fy, 74.45.+c, 73.23.-b

Manifestations of the proximity effect in the electron transport of the hybrid normal metal-superconductor (NS) structures are in the focus of current extensive research. Up to now the electric conductance in NS-hybrids has been receiving much more attention than thermal conductance; the imbalance can be ascribed to difficulties one encounters in carrying out thermal transport experiments in mesoscopic samples. A remarkable breakthrough in recent measurements [1, 2] of both the thermal conductance and thermopower in an *Au* (N) diffusive wire of the micron length and submicron cross-size and thickness, where an *Al* (S) needle-like sample of similar parameters is deposited across it, as shown in Fig. 1,a, calls for and motivates a detailed theoretical investigation of heat and charge transport in mesoscopic NS-hybrids. In our Letter we develop a theory of thermal and electric conductances in mesoscopic proximity structures in the diffusive limit, which, as we show below, describes the experimental situation. We find that while the electric conductance exhibits the conventional reentrance behavior, the thermal conductance rapidly decreases with temperature, as $\kappa \sim T^4$, in a qualitative agreement with experimental findings.

Experiments [1, 2] showed a tiny (within a few percents) change in the electric conductance of *Au* due to the proximity effect in accordance with the past studies. The thermal conductance, in a contrast, dropped with temperature decreasing, by the order of magnitude as compared to its value $\kappa_N(T)$ in the normal state. This result seems to excellently follow the original idea by Andreev [3] first applied to the thermal conductance of the intermediate state of a superconductor [4]: If the interface resistance is negligibly small, and the wire thickness is smaller than the coherence length ξ_0 , then the sandwich-like NS contact in Fig. 1,a can be modelled by an inset of the superconductor into the N-wire, Fig. 1,b. Then the superconductor lead in Fig. 1,b plays the role of a quantum barrier for normal quasiparticles with the energies E smaller than the superconducting order parameter Δ . Low-energy electrons hit the barrier and convert

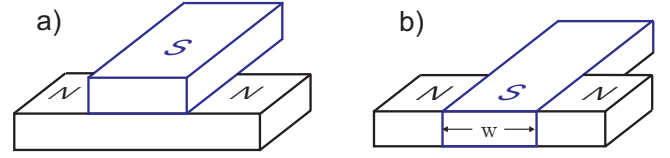


FIG. 1: Two models of the NS interface: sandwich geometry (a), and inset geometry (b).

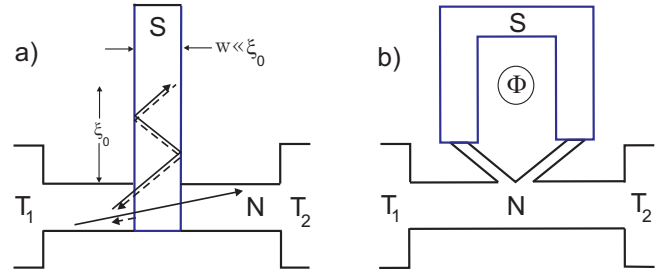


FIG. 2: (a) Upper view of the model of the NS interface in Fig. 1, with the ballistic trajectories of the electrons (solid lines) and holes (dashed lines); (b) the geometry of house-like Andreev interferometer with the magnetic flux Φ .

into the retro-reflected holes (Andreev reflection), carrying the same energy back in the opposite direction. Thus, the subgap thermal flow through the superconductor is blocked, and only quasiparticles with energies $E > \Delta$ participate in the heat transport. At low temperatures, $T \ll \Delta$, the thermal conductance follows nearly exponential temperature dependence, $\kappa \sim T \exp(-\Delta/T)$ [3], used in Ref. 2 for data fitting.

Given a very satisfactory fit, the above line of reasoning would have been conclusive, unless the disturbing observation that in the experiments of [2], the cross size w of the N- and S-leads was considerably smaller than ξ_0 , making the Andreev barrier semi-transparent for the subgap particles. This raises serious doubts about the applicability of the above ‘macroscopic’ consideration, requiring $w \gg \xi_0$, to the quantum problem, $w < \xi_0$, where the subgap quasiparticles may well dominate the thermal conductance at low temperatures. This is the case in bal-

listic structures, with the elastic scattering length ℓ much larger than ξ_0 and w , where the heat flow is carried by quasiparticles traversing the proximity region and overcoming the weak Andreev barrier (see Fig. 2,a). Such effect was considered within a model of a small S-inclusion in the ballistic N-wire [5]. In the geometry of Fig. 2,a, the quasiparticles which propagate into the S-lead over the distance ξ_0 , undergo complete Andreev reflection, and sink out from the heat transport [6]. In the limit of almost transparent Andreev barrier, $w \ll \xi_0$, the ratio κ/κ_N in the ballistic structure is basically determined by the interface geometry and therefore should be temperature independent, except in a vicinity of T_c , where, as ξ_0 becomes larger than the length of the S-lead, the Andreev reflection is suppressed, and κ returns to κ_N .

In this Letter, we focus on the diffusive limit, $\ell \ll (w, \xi_0)$, that describes the experimental situation in Refs. 1, 2 and reveals a wealth of interesting physics. In this case, due to multiple coherent backscattering of electrons by the impurities within the proximity region [7], the number of Andreev reflected quasiparticles effectively enhances. This enhancement becomes especially pronounced as the energy approaches zero, and, correspondingly, the size $\xi_N(E) = \sqrt{\hbar\mathcal{D}/2E}$ of the proximity region in a normal metal with the diffusion coefficient \mathcal{D} infinitely increases. This effect is known as the reason for the zero-bias conductance peak in NS structures with an opaque interface [8]. In our context, enhanced Andreev reflection means the suppression of the heat flow at small energies even for the weak Andreev barrier, $w \ll \xi_0$, and, as we show below, results in a rapid decrease of κ/κ_N with temperature as observed in the experiment. Furthermore, the temperature dependence of κ appears to be power-like rather than the exponential, in contrast to the model of the “impenetrable” Andreev barrier [2, 3] which blocks the heat transport within the entire sub-gap region. Due to high sensitivity of the heat flow to the proximity effect, one can also expect essential dependence of the thermal conductance on the order parameter phase difference ϕ applied to the proximity structure (in the ballistic case, such dependence was predicted in Ref. 5). A hallmark of the phase-coherent heat transport was found in thermopower measurements [1, 9].

We consider both electric and thermal conductances of the proximity structure in Fig. 2,a in a diffusive limit, assuming the N-lead of length L_N ($-L_N/2 < x < L_N/2$) to be connected to normal reservoirs, and the S-lead of length L_S ($0 < y < L_S$) attached to the middle of the N-lead. In such geometry, the quasiparticle flow along the S-lead is blocked, and therefore the quasiparticle distribution in this lead is spatially uniform. For this reason, it is enough to solve one-dimensional diffusive kinetic equations [8, 10] for the distribution functions f_{\pm} in the N-lead, $\partial_x(D_{\pm}\partial_x f_{\pm}) = 0$, neglecting spatial variations across the leads at $w \ll \xi_0$. The diffusion coefficients D_{\pm} are defined through the retarded branch of the spectral

angle θ as $D_+ = \cos^2 \text{Im } \theta$ and $D_- = \cosh^2 \text{Re } \theta$. The spectral angles θ_N and θ_S in the N- and S-lead, respectively, are to be determined from the Usadel equation

$$2(E \sinh \theta - \Delta \cosh \theta) = i\hbar\mathcal{D}\partial^2\theta, \quad (1)$$

with the boundary conditions $\theta_N = 0$ at the normal reservoirs, and $\partial_y\theta_S = 0$ at the edge of the S-lead. At the transparent NS interface, the spectral angle is continuous, $\theta_N(0) = \theta_S(0) \equiv \theta_0$, and obeys the current conservation law [11], $g_S\partial_y\theta_S(0) = \pm 2g_N\partial_x\theta_N(\mp 0)$, where $g_{N,S}$ are the conductances of the leads per unit length.

The kinetic equations have the first integral,

$$D_{\pm}\partial_x f_{\pm} = I_{\pm}(E), \quad (2)$$

where the spatial constants I_{\pm} , which have the meaning of the spectral densities of the probability and electric currents, respectively, are to be determined from the boundary conditions for f_{\pm} . The electric current I and the thermal flow Q in the N-lead are related to I_{\pm} as

$$I = \frac{g_N}{e} \int_0^{\infty} I_-(E) dE, \quad Q = \frac{g_N}{e^2} \int_0^{\infty} EI_+(E) dE. \quad (3)$$

The thermal flow arises at different temperatures T_1 and T_2 of the N-reservoirs, which imposes the boundary conditions for the quasiparticle density function $f_{\pm}(\mp L_N/2) = \tanh(E/2T_{1,2})$, where a small thermopower is neglected. Assuming the temperature difference to be small, $T_1 - T_2 \ll T = (T_1 + T_2)/2$, Eqs. (2) and (3) give the expression for the thermal conductance,

$$\kappa = \frac{Q}{L_N(T_1 - T_2)} = \frac{3\kappa_N}{2\pi^2 T^3} \int_0^{\infty} \frac{E^2 R_Q^{-1}(E) dE}{\cosh^2(E/2T)}, \quad (4)$$

where $R_Q(E) = \langle D_+^{-1}(E, x) \rangle$ is the dimensionless spectral thermal resistance, and the angle brackets denote average over the length of the N-lead.

In the problem of charge transport, we assume the left and right reservoirs to be voltage biased at $\mp V/2$ and maintained at equal temperature T , which results in the boundary condition for the charge imbalance function f_- ,

$$f_-(\pm L_N/2) = \frac{1}{2} \left[\tanh \frac{E \pm eV/2}{2T} - \tanh \frac{E \mp eV/2}{2T} \right]. \quad (5)$$

Using Eqs. (2), (3) and (5), we obtain the zero-bias conductance of the N-wire,

$$G = \frac{dI}{dV} \Big|_{V \rightarrow 0} = \frac{G_N}{2T} \int_0^{\infty} \frac{R_I^{-1}(E) dE}{\cosh^2(E/2T)}, \quad (6)$$

where $G_N = g_N/L_N$ is the normal conductance, and $R_I(E) = \langle D_-^{-1}(E, x) \rangle$ is the spectral electric resistance.

The calculation of the spectral angle $\theta_N(E, x)$, which enters the coefficients D_{\pm} , is to be performed numerically.

However, neglecting spatial variations in Δ within the proximity region (that may result in some non-crucial numerical factors at most) and assuming the lengths of the leads to be much larger than the characteristic scales $\xi_{N,S}$ of spatial variation of the spectral angle,

$$L_N \gg \xi_N = \sqrt{\frac{\hbar \mathcal{D}_N}{2E}}, \quad L_S \gg \xi_S = \sqrt{\frac{\hbar \mathcal{D}_S}{2\sqrt{\Delta^2 - E^2}}}, \quad (7)$$

one can apply the following analytical solutions of Eq. (1) for the structure with semi-infinite leads,

$$\tanh \frac{\theta_N(E, x)}{4} = \tanh \frac{\theta_0(E)}{4} e^{-|x|/\xi_N \sqrt{i}}, \quad (8)$$

$$\tanh \frac{\theta_S(E, x) - \theta_B}{4} = \tanh \frac{\theta_0(E) - \theta_B}{4} e^{-y/\xi_S}, \quad (9)$$

$$\theta_0 = \ln \frac{\sqrt{E + \Delta} + \sqrt{Er}}{\sqrt{E - \Delta} + \sqrt{Er}}, \quad r = \frac{4\mathcal{D}_S}{\mathcal{D}_N} \left(\frac{g_N}{g_S} \right)^2 \sim \frac{\mathcal{D}_N}{\mathcal{D}_S}. \quad (10)$$

Here $\theta_B = \text{Arctanh}(\Delta/E)$ is the spectral angle in a bulk superconductor, and the parameter r determines the strength of the proximity effect (see comments to Fig. 3). Similar solution for the normal part of a long SNS structure was used in Ref. 12.

The semi-infinite-lead approximation enables us to estimate the magnitude of κ in the most interesting case of small temperatures, $T \ll \Delta$. Although the coefficient D_+ is suppressed within the whole proximity region, $|x| \lesssim \xi_N \sim \xi_0 \sqrt{\Delta/T}$, the contribution δR_Q of this region to the thermal resistance R_Q comes from the narrow (of the order of $\xi_0 = \sqrt{\hbar \mathcal{D}_N / 2\Delta}$) vicinity of the crossing point, in a contrast to the proximity correction to the zero-bias electric conductance which is formed over the much larger scale ξ_N . Within this region, the coefficient D_+ is anomalously small and turns to zero at $E \rightarrow 0$,

$$D_+ \approx (E/\Delta) (|x|/\xi_0 + \sqrt{r})^2, \quad (11)$$

which results in the following estimate of δR_Q at the characteristic energies $E \sim T$,

$$\delta R_Q(T) \approx T_0/T, \quad T_0 = \Delta \xi_0 / L_N \sqrt{r}. \quad (12)$$

Thus, at $T < T_0$, the proximity region dominates the net thermal resistance giving rise to the power-like decrease of $\kappa \sim \kappa_N T/T_0 \sim T^4$ with T . At very low temperatures, smaller than the Thouless energy $E_{\text{Th}} = \hbar \mathcal{D}_N / L_N^2$, the N-reservoirs begin to affect the quasiparticle spectrum at the contact area, and the approximation of semi-infinite N-lead fails. In this case, E_{Th} provides the cutoff in the decrease of the coefficient D_+ at small E , which therefore saturates at $D_+ \sim E_{\text{Th}}/\Delta$. As the result, the thermal conductance at $T < E_{\text{Th}}$ starts to decrease slower, as $\kappa_N \sim T^3$, with a small prefactor $E_{\text{Th}}/T_0 \sim \xi_0 \sqrt{r}/L_N$. At the same time, the electric conductance shows behavior typical for the proximity structures: as T decreases, $G(T)$ approaches maximum and then returns to G_N .

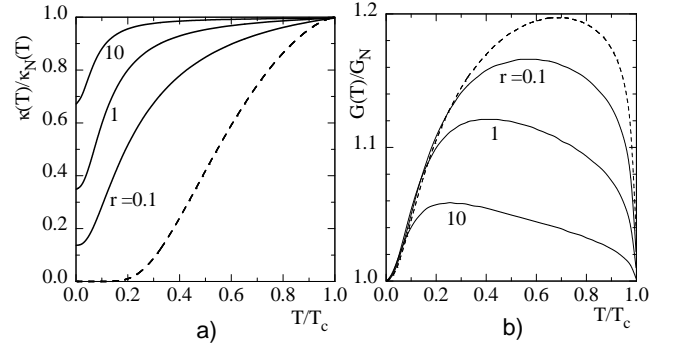


FIG. 3: Temperature dependencies of κ/κ_N (a) and G/G_N (b) obtained by numerical solution of Eq. (1), in comparison with the Andreev model (dashed curves), at $L_N = 10\xi_0$.

Shown in Fig. 3 are the results of calculation of thermal and electric conductances within the whole relevant temperature region $0 < T < T_c$ for different magnitudes of the parameter r . If the conductivity of the N-lead is small, $r \ll 1$, the spectrum within the S-lead is almost unperturbed [$\theta_0 \approx \theta_B$, see Eq. (10)], and the crossing area plays the role of a superconducting reservoir. In terms of quasiparticle motion, quasiparticles ‘would prefer’ to diffuse into the high-conductive S-lead, where most of them undergo Andreev reflection thus additionally reducing κ and increasing G . In the opposite limit, $r \gg 1$, the quasiparticles avoid penetration into the low-conductive S-lead, which suppresses the proximity effect ($\theta_0 \rightarrow 0$), and, correspondingly, enhances κ and reduces the peak in $G(T)$. Note that for all reasonable values of r , our quantum model gives the magnitude of κ considerably larger than that due to the classic model [2, 3].

The high sensitivity of thermal conductance to the details of the quasiparticle spectrum can be used for a study of the effects of phase coherence in the mesoscopic devices known as Andreev interferometers. Usually, the interferometer circuits contain a superconducting loop with the order parameter phase difference ϕ controlled, e.g., by the magnetic flux, and connected to an SNS junction. The electric conductance of the junction (or the N-wire attached to the junction) depends periodically on ϕ .

The basic features of the phase-coherent heat transport in the proximity structures can be demonstrated within the model of the ‘‘house interferometer’’ [1, 2] shown in Fig. 2.b. Assuming the length of the junction arms to be smaller than ξ_0 , and the normal conductivity of the S-loop to be much larger than the conductivity of the N-wire, one can neglect the change in the junction quasiparticle spectrum due to proximity to the N-wire. In this limit, the spectrum at the contact area is similar to the BCS-like spectrum of a separate short diffusive SNS junction, with the phase-dependent energy gap $E_g(\phi) = \Delta |\cos(\phi/2)|$ [13]. This implies that the contact area behaves as an impenetrable Andreev barrier with the phase-dependent height $E_g(\phi)$, and therefore

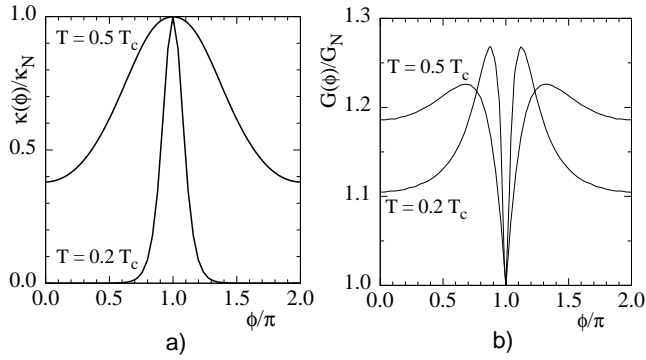


FIG. 4: Phase dependencies of the thermal (a) and electric (b) conductances in the geometry of house interferometer in Fig.2,b, for different temperatures ($L_N = 10\xi_0$).

the heat transfer is governed by the quasiparticles with the energies $E > E_g(\phi)$. Within this region, we apply Eq. (4), thus taking into account spatial variations in the diffusion coefficient D_+ within the proximity region. These variations are a diffusive analog [14] of the ballistic over-the-barrier Andreev reflection from a rapidly varying order parameter potential.

The phase dependence of the thermal conductance is presented in Fig. 4,a. Due to Andreev reflection from the contact area, κ is generally suppressed, according to the mechanism discussed above. However, as the phase difference approaches odd multiples of π , the energy gap E_g closes, and all quasiparticles freely diffuse through the N-wire, which restores the normal value of κ . Thus, at low temperatures, $\kappa(\phi)$ exhibits strong oscillations with the phase ϕ , with sharp peaks at $\phi \bmod 2\pi = \pi$. The electric conductance shows oscillations with sharp dips at the same points, but with much lower amplitude (Fig. 4,b).

In conclusion, we have developed a theory of the heat transport through the normal part of diffusive NS nanostructures. The Andreev reflection from the NS interface blocks the quasiparticle probability current, and therefore the heat flow through the normal wire, coupled with the superconductor over a small area, is essentially suppressed. Our approach takes into account self-consistently the influence of both the normal metal and superconductor on the quasiparticle spectrum within the proximity region, extending thus the ballistic concept of partial Andreev reflection from the superconductor of finite width to diffusive proximity systems. The important feature of the diffusive structures is the essential enhancement of the Andreev reflection probability at low energies due to multiple returns of coherent quasiparticles to the contact area. For this reason, the proximity region dominates the net thermal resistance of a long normal wire with the length $L_N \gg \xi_0$ at low temperatures, even if the size of the contact area is much smaller than the coherence length ξ_0 . This results in a power-law decrease in the thermal conductance with the temperature, $\kappa \sim T^4$, transforming into a cubic law at the tem-

peratures smaller than the Thouless energy. The effect becomes more pronounced when the carriers mobility in the superconductor is higher than in the normal metal. If the wire is attached to the SNS junction with the order parameter phase difference ϕ between the electrodes, the thermal conductance reveals full-scale oscillations with ϕ and shows large peaks at odd multiples of π .

In the experiments [2], the results of measurements of $\kappa(T)$ were fitted by the Andreev formula [3], which assumes complete blockade of the thermal flow within the entire subgap region, $E < \Delta$, and therefore leads to the exponential temperature dependence of κ . Although this fitting looks satisfactory, the physical background for the applicability of such a simple model remains unclear, because of the small width $w \approx 0.4\xi_0$ of the wires and unavoidable suppression of electron-hole correlations in the S-wire within the proximity region. This calls for further investigations, including independent measurements of $\kappa(T)$ in the normal state and the extension of theoretical calculations for rather complicated geometry of real proximity structure in Ref. 2.

It is a pleasure to thank V. Chandrasekhar, Yu. M. Galperin, V. I. Kozub, A. N. Shelankov, and V. S. Shumeiko for fruitful discussions. This work was supported by the U.S. Department of Energy, Office of Science under contract No. W-31-109-ENG-38.

-
- [1] J. Eom, C.-J. Chien, and V. Chandrasekhar, Phys. Rev. Lett. **81**, 437 (1998).
 - [2] D. A. Dikin, S. Jung, and V. Chandrasekhar, Phys. Rev. B **65**, 012511 (2001).
 - [3] A. F. Andreev, Sov. Phys. JETP **19**, 1228 (1964).
 - [4] N. V. Zavaritskiĭ, Sov. Phys. JETP **11**, 1207 (1960).
 - [5] N. R. Claughton and C. J. Lambert, Phys. Rev. B **53**, 6605 (1996).
 - [6] We note that Andreev reflection, due to its quantum nature, develops continuously at the scale of ξ_0 , and therefore the picture of instantaneous electron-hole conversion in Fig. 2,a is rather conditional.
 - [7] B. J. van Wees, P. de Vries, P. Magne , and T. M. Klapwijk, Phys. Rev. Lett. **69**, 510 (1992).
 - [8] A. F. Volkov and T. M. Klapwijk, Phys. Lett. A **168**, 217 (1992); A. F. Volkov, A. V. Zaitsev, and T. M. Klapwijk, Physica C **210**, 21 (1993).
 - [9] D. A. Dikin, S. Jung, and V. Chandrasekhar, Europhys. Lett. **57**, 564 (2002); A. Parsons, I. A. Soshnin, and V. T. Petrashov, Phys. Rev. B **67**, 140502(R) (2003).
 - [10] J. Rammer and H. Smith, Rev. Mod. Phys. **58**, 323 (1986); T. H. Stoof and Yu. V. Nazarov, Phys. Rev. B **53**, 14496 (1996).
 - [11] Yu. V. Nazarov, Phys. Rev. Lett. **73**, 1420 (1994); Superlattices Microstruct. **25**, 1221 (1999).
 - [12] A. D. Zaikin and G. F. Zharkov, Sov. J. Low Temp. Phys. **7**, 375 (1981).
 - [13] I. O. Kulik and A. N. Omelyanchouk, Sov. J. Low Temp. Phys. **5**, 296 (1978).
 - [14] E. V. Bezuglyi, E. N. Bratus', V. S. Shumeiko, G. Wendin, and H. Takayanagi, Phys. Rev. B **62**, 14439 (2000).